Melting Line of Graphite

A. M. Kondratyev and A. D. Rakhel[*]

Joint Institute for High Temperatures, Izhorskaya 13, Bld. 2, Moscow 125412, Russia

(Received 29 September 2018; published 3 May 2019)

A thin plate of highly oriented pyrolytic graphite (HOPG) with the hexagonal axis (c axis) perpendicular to its surface was sandwiched between two plates of the window material and heated by an electric current pulse. The quasistatic heating process has been affected, in which the graphite sample undergoes thermal expansion only along the c axis and is melted at a pressure of 0.3–2 GPa. The set of thermodynamic quantities characterizing completely the thermodynamic states of the sample in such a process (specific volume, enthalpy, temperature, and pressure) as well as the electrical resistivity, were measured with an uncertainty <5%. It has been found that under the above pressures the HOPG melts at the temperatures of 6.3 to 6.7 kK, which are substantially higher than the literature values derived from indirect measurements. The jumps in the volume, resistivity and enthalpy of carbon on melting have been determined as well as values of the isochoric heat capacity and the sound velocity of the graphite and liquid carbon. The heat capacities in the vicinity of the melting line turned out to be close to the Dulong-Petit value while the sound velocity of liquid carbon clearly demonstrates an increase with volume indicating a change from the planar sp^2 to tetrahedral sp^3 covalent bonding.

Introduction.—The location of the melting line of graphite on the phase diagram of carbon, as well as the thermophysical properties of graphite and liquid carbon in the vicinity of the line, are of interest in such technologies as the fabrication of artificial diamonds, in the applications of graphite as a high-temperature structural and ablating material, for understanding of different physical phenomena in geophysics and astronomy, and in the designing of the fusion capsule for the National Ignition Facility [1–3]. It is worth noting here that liquid carbon is of special interest due to the expectations of the liquid-liquid phase transition in this network-forming fluid [4,5].

Despite the substantial efforts made to explore the phase diagram of carbon, the location of the melting line is still poorly known and the electronic properties of graphite and liquid carbon in the vicinity of the line are not well understood [2,3,6]. Experimental data on the properties are scarce and very uncertain because of the high required pressures and temperatures. The present knowledge of the phase diagram of carbon is almost entirely based on the molecular-dynamics (MD) simulations [2–8] and the phenomenological model [1,9,10] parameters of which are fitted to the available experimental data and the MD simulation results.

Since fractions of the sp^1, sp^2, and sp^3 sites in carbon change when the thermodynamic state is varied [2], it is very difficult to construct a correct interatomic potential for the MD simulations. The simulations in this case should be *ab initio*. At present the quantum-mechanical description of the condensed state is usually affected by means of the finite temperature density functional techniques [2,3,7,8].

However, since the latter utilize certain approximations, it is very important to compare the simulation results with accurate experimental data for a particular system.

The melting line of graphite [11] has been deduced from the estimates of the heat of fusion [12] by extrapolating the low pressure heat capacity values [13] to the essentially higher pressures. In Ref. [12] the spectroscopic graphite was investigated by compressing in the high-pressure cell and heating by an electric current pulse during ∼1 ms. For such an experiment it is very difficult to perform a uniform heating of the sample whose deformation is not controlled. An accurate estimate of the heat losses from the sample to the cell walls also presents a serious problem [12]. An attempt to measure directly the melting temperature of graphite in the high-pressure cell had been made in Ref. [14]. However, those results are very uncertain since no clear interpretation of the effect of diffusion of carbon from the sample into the environment on the temperature measurements was given.

The temperature and enthalpy of graphite at the pressures $P = 0.1$–0.2 GPa have been measured in Ref. [13]. Only the beginning of melting of the graphite samples was identified in the experiments [15]. The end of melting could not be detected due to the difficulty of maintaining the initial shape of the samples in the experiments [13,15]. The uncontrolled deformation of the samples had a strong influence on the temperature measurements as well as the effect of a plume of carbon, which formed near the surface of the samples [16].

The pulsed heating of the graphite samples placed in thick capillary tubes with calibrated bores allowed the

authors [17] well-pronounced melting plateaus to be observed with the temperature values of 5.4–6.0 kK. However, neither the samples' volume nor pressure was measured in the experiments [17], so that enthalpy, density, and pressure were estimated with some not precisely known errors.

This Letter reports the complete set of thermodynamic quantities (necessary to determine the Gibbs free energy) as well as the electrical resistivity data measured for graphite and liquid carbon in a broad vicinity of the melting line.

Experimental.—The HOPG sample (a plate of 20–40 μm thickness, of 4.5–5.0 mm width and 10 mm length) with the c axis perpendicular to the surface of the plate was sandwiched between two plates of the window material and this assembly was glued together with a transparent glue. The term window material designates a transparent material with known mechanical and optical properties. For these experiments we used silica glass or sapphire plates of 3–5 mm thickness, 10 mm width and length. Parallelism of the polished surfaces of the plates was better than 3 μm per 10 mm. Such a sample can be uniformly heated by an electric current pulse and a one-dimensional thermal expansion of the sample can be affected. A uniform heating was achieved by using a sufficiently thin sample (that made the skin effect to be negligible). Since the heating power varied sufficiently slowly with time the heating was a quasistatic process, so that both density and pressure were uniform throughout the sample [18,19].

A uniform distribution of temperature was maintained due to a sufficiently fast heating and placing a thin layer of glue (polymethyl methacrylate of about 1 μm thickness) between the sample and the window plates. In this case a uniform temperature distribution was only slightly perturbed in a thin layer near the sample surface with a thickness $\delta \approx \sqrt{\chi t_T}$, where χ is the thermometric conductivity of graphite, and t_T is the temperature rise time [20]. For graphite $\chi \approx 10^{-2}$ cm^2 c^{-1} (along the c axis) so that when $t_T = 10^{-7}$ s, $\delta \approx 0.3$ μm; the thickness of the heated layer of the glue is $\sim$0.1 μm.

We used samples of HOPG supplied by "Atomgraf AG" Ltd. This graphite had a purity of 99.999% (by mass), normal density of 2.26 g cm^{-3}, and normal resistivity along the basal planes of 0.44 $\mu\Omega$ m. In each experiment we measured the current through the sample (by a current transformer), the voltage drop across it (by a resistive voltage divider), its volume and pressure (by a laser interferometer), and temperature (by a brightness pyrometer, see Fig. 1).

For the measurement of the volume the displacement of the sample surface caused by the thermal expansion was detected. A laser beam with a wavelength of 1550 nm was incident normally on the experimental assembly (as shown in Fig. 1). The beam was partially reflected from the free surface of the window plate and formed a reference beam, and partially it was reflected from a dielectric mirror
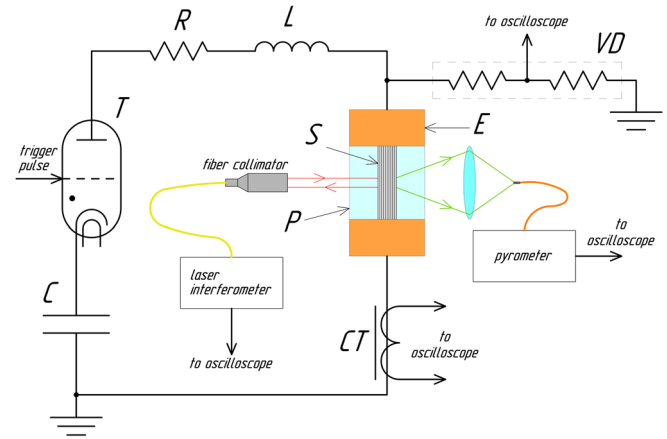

FIG. 1. Schematic diagram of the experiments. The HOPG sample (S) is placed between two plates of the window material (P is the left plate) and two electrodes (E is the high-potential electrode). To heat the sample the electric circuit is used which contains a capacitor (C), a ballast resistor (R), an inductance (L) and a current switch (T).

deposited on the opposite surface of the plate which was in contact with the sample. The two beams were superimposed on each other and the intensity of the interference was recorded using a high-speed light sensor and an oscilloscope. Because of the thermal expansion of the sample the window plate was compressed by it and the optical paths lengths of the beams were changed, which caused a change in the intensity. The temporal dependence of the intensity can be related to that of the sample surface displacement and hence the volume [18,19]. The procedure of determining the pressure is based on the measurements of the sample surface displacement and the knowledge of the equation of state of the window material. The task is reduced in this case to determining the pressure at a piston, which moves according to a known law in a medium with a known equation of state. The equation of state data for sapphire and silica glass can be found in Ref. [21].

The pyrometry technique is based on the assumption that the thermal radiation emitted of the sample has the characteristic black-body spectrum modified by a wavelength and temperature dependent emissivity. The radiation from a circular target area on the sample surface with a diameter of 2 mm was focused by a lens on the end face of an optical fiber. At the opposite end of the fiber the radiation was collimated, sent through an interference filter, and focused onto a photodetector. We used two interference filters centered at the wavelength of 656 and 850 nm (both with FWHM = 10 nm). The temperature values were determined from the brightness records by using the temperature tie point $T = 4.16$ kK at the enthalpy value of 96 kJ mol^{-1} [22,23], assuming the emissivity to be constant.

We have carried out 20 experiments on graphite. Figure 2 shows the measured dependencies of the pressure on density for some of these experiments.
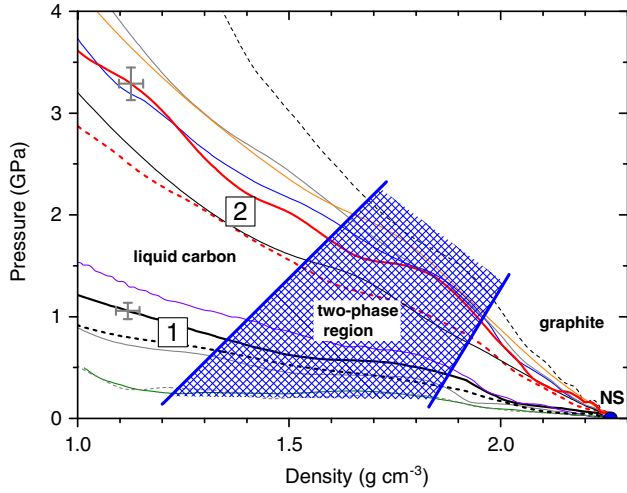
FIG. 2. The experimental paths in the pressure-density plane which go from the normal state (NS). The hatched area designates the melting region; the two pairs of the experiments indicated with the thick red and black lines (solid and dashed) represent the experiments with relatively low pressures (1) and the higher pressures (2). The error bars show uncertainties of our measurements.

In Fig. 3 the measured quantities are plotted as functions of temperature for the four representing experiments indicated in Fig. 2. In the two experiments that are shown with the red solid and black dashed line we used the interference filter at the wavelength of 850 nm, while in the other two experiments the measurements were accomplished with the 656 nm filter. In the experiments that are shown with the black lines the samples were sandwiched between silica glass plates, while in the other two

experiments sapphire plates were used. From Fig. 3(a) it follows that our results are in good agreement with the data [15,22,23]. The accuracy of our temperature measurements is also demonstrated by the measured dependencies of the density of graphite on temperature. As seen from Fig. 3(c), these dependencies agree well with the reference data [24,25] and attest that there are no jumps or kinks near the temperature tie point. Figure 3(b) shows that the same is true for the dependencies of the resistivity. In Figs. 3(b), 3(c) the temperature values below the tie point were obtained from the measured enthalpy values by using the heat capacity values of Ref. [23]. All the data presented in Figs. 2, 3 can be found in a table form in the Supplemental Material [26].

From Fig. 3 it follows that in the range $T = 6.3$–6.7 kK the dependencies have well-pronounced melting plateaus. The presence of the plateaus allows us to determine accurately the temperature of the beginning and end of melting as well as the jumps of the quantities on melting.

Using the present data, we have also determined a segment of the melting line of graphite in the PT plane. As seen from Fig. 4, the present temperature values on the melting line are essentially higher than those of the measurements [11,14,28] and the theoretical predictions [4,6,29].

We have verified that the melting line obtained here has a slope that agrees with the Clapeyron-Clausius equation:

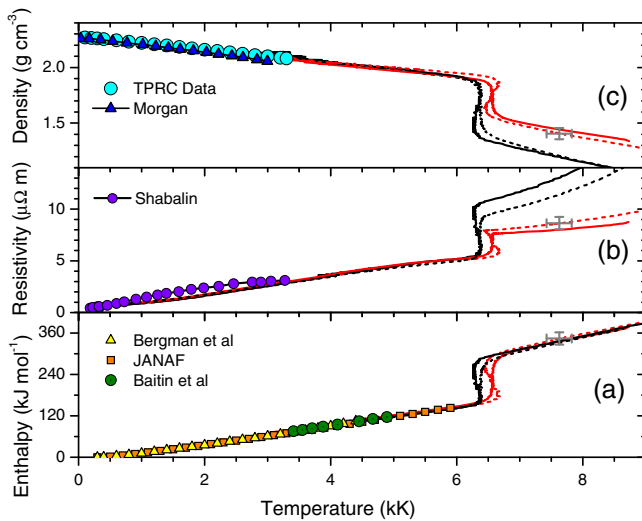$$\frac{d \ln T_m}{dP} = \frac{V_l - V_g}{Q_m}, \qquad (1)$$

FIG. 3. The temperature dependencies of enthalpy (a), resistivity (b), and density (c), measured in four experiments of this work (black and red lines) are compared with the literature data [15,22–25,27]. The error bars show uncertainties of our measurements. The notations of the lines are the same as in Fig. 2.
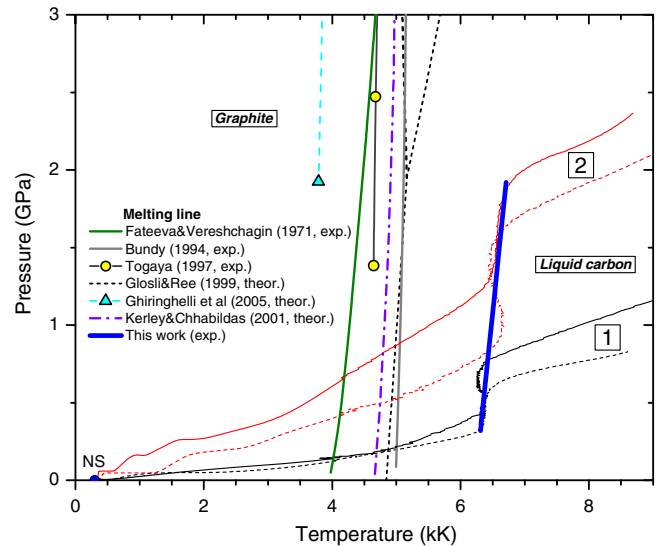

FIG. 4. Segment of the melting line of graphite determined in this work (thick blue line) is compared with that of Ref. [14] (green line), [11] (gray solid line), [28] (yellow circles), [4] (black short dashed lines), [6] (blue triangle), [29] (violet dashed dotted line); the dependencies measured in our four experiments (1,2) are shown with the thin lines which go from the normal state.

where T_m is the melting temperature, V_g and V_l are the molar volumes of graphite and liquid carbon at melting, and Q_m is the molar heat of fusion of graphite. We found that the derivative on the left-hand side of Eq. (1), for which we obtained a value of 0.038 GPa^{-1}, differs from the right-hand side ratio by less than 15%.

We have also checked that for all our experiments the start of melting determined from the pyrometer signal agrees with those determined from the interferometer and the voltage divider signals. The singularity associated with the start of melting in the voltage signal is discussed in Refs. [18,19]. The singularity caused by melting in the thermal expansion was manifested as a kink in the dependence of the sample surface displacement on the heat dissipated in the sample. This verification suggests that the temperature in the optical skin-layer from which the thermal radiation is emitted (and detected by the pyrometer) differs only slightly from that in the bulk of the sample; estimates show that the difference does not exceed 100 K.

From the present data we determined the heat capacity values for graphite and liquid carbon. The isochoric heat capacity was calculated using the definition $C_V = (\partial Q/\partial T)_V$, where Q is the molar heat dissipated in the sample. For graphite in the temperature range of 4–6 kK we obtained the value $C_{V,g} = (3.3 \pm 0.3)R$, where R is the gas constant. Since the electron contribution to the heat capacity of graphite is small [10,30], and the temperature values from the above range exceed the Debye temperature, it follows that for graphite the Dulong-Petit law is satisfied. For liquid carbon we found the value $C_{V,l} = (3.8 \pm 0.4)R$, which remained nearly constant over the entire region of the liquid state investigated.

We have also determined the molar entropy

$$S = S_0 + \int_0^Q \frac{dQ'}{T} \qquad (2)$$

(S_0 is the normal value) and the Gibbs free energy

$$G = W - TS, \qquad (3)$$

where W is the molar enthalpy. In so doing we obtained the dependencies of $G(P,T)$ along the paths of our experiments in the PT plane. In order to check self-consistency of these results we determined the melting temperature values from the condition of equilibrium: $G_g(P,T) = G_l(P,T)$. It has been found that the melting temperature values obtained in this way agree with those presented in Fig. 4 to within 6%.

From the present data the velocity of sound can be determined [31]. We revealed that along the isobar $P = 1$ GPa the sound velocity of liquid carbon increases monotonically with decreasing density from a value of 2.3 $km\,s^{-1}$ near the melting line to a value of 3.5 $km\,s^{-1}$ at a density of 1 $g\,cm^{-3}$. Such behavior seems to indicate an
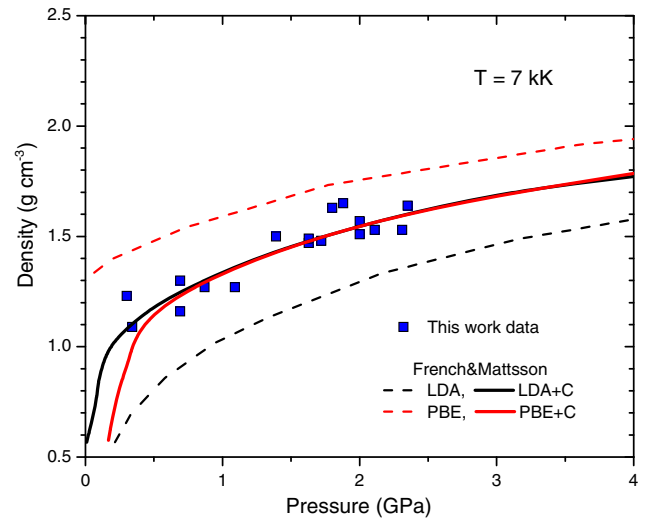

FIG. 5. Density of liquid carbon as a function of pressure along the isotherm $T = 7$ kK. Density values determined in these experiments (marks) are compared with the MD simulations results [32] performed using the local density approximation (black dash line) and the PBE functional [33] (red dashed line); the empirically corrected MD results are shown with the solid lines.

increase in the fraction of the tetrahedral sp^3 sites in the expanded liquid carbon [2,6,7]. It should be noted that in the above density range the enthalpy values are noticeably lower than the heat of sublimation of carbon of 715.5 $kJ\,mol^{-1}$ [30] [see Fig. 3(a)].

Comparison with the MD simulations results.—In Ref. [32] the *ab initio* MD simulations have been performed for liquid carbon. In Fig. 5 we compare the dependencies of density on pressure computed in [32] with our results. As follows from this figure, our results agree to within the experimental uncertainty (which is of the order of the scatter of the data points) with the *ab initio* MD simulations results only in the case the latter are empirically corrected in order to get the correct values of the normal density and bulk modulus of graphite [32].

Uncertainties.—Experimental errors of the measured physical quantities are indicated in Figs. 2, 3. The errors in the present pressure measurements shown in Fig. 2 include the error of the interferometric measurements of the sample surface displacement ($<4\%$) and the error in the equation of state of the window material [21] used to relate the displacement with the pressure. The error of the present temperature measurements shown in Fig. 3 was estimated taking into account the scatter in the results obtained for different interference filters, the window materials, glues (used to bond the assembly), and at different heating rates (which were varied by an order of magnitude). The error includes also the error in the tie temperature value and that arises due to the change in emissivity observed in Ref. [15].

*rakhel@oivtran.ru

[1] L. E. Fried and W. M. Howard, Phys. Rev. B **61**, 8734 (2000).

[2] G. Galli, R. M. Martin, R. Car, and M. Parrinello Phys. Rev. B **42**, 7470 (1990).

[3] A. A. Correa, L. X. Benedict, D. A. Young, E. Schwegler, and S. A. Bonev, Phys. Rev. B **78**, 024101 (2008).

[4] J. N. Glosli and F. H. Ree, Phys. Rev. Lett. **82**, 4659 (1999).

[5] M. Wilson, J. Phys. Condens. Matter **28**, 503001 (2016).

[6] L. M. Ghiringhelli, C. Valeriani, J. H. Los, E. J. Meijer, A. Fasolino, and D. Frenkel, Mol. Phys. **106**, 2011 (2008).

[7] X. Wang, S. Scandolo, and R. Car, Phys. Rev. Lett. **95**, 185701 (2005).

[8] V. S. Dozhdikov, A. Yu. Basharin, P. R. Levashov, and D. V. Minakov, J. Chem. Phys. **147**, 214302 (2017).

[9] A. M. Molodets, M. A. Molodets, and S. S. Nabatov, Combust Explos. Shock Waves **36**, 240 (2000).

[10] M. van Thiel and F. H. Ree, Phys. Rev. B **48**, 3591 (1993).

[11] F. P. Bundy, W. A. Basset, M. S. Weathers, R. J. Hemley, H. K. Mao, and A. F. Goncharov, Carbon **34**, 141 (1996).

[12] M. Togaya, S. Sugiyama, and E. Minuhara, AIP Conf. Proc. **309**, 255 (1994).

[13] M. A. Scheindlin and V. N. Senchenko, Sov. Phys. Dokl. **33**, 142 (1988).

[14] N. S. Fateeva and L. F. Vereshchagin, Pis'ma Zh. Eksp. Teor. Fiz. **13**, 157 (1971) [JETP Lett. **13**, 110 (1971)].

[15] A. V. Baitin, A. A. Lebedev, S. V. Romanenko, V. N. Senchenko, and M. A. Scheindlin, High Temp. High Press. **22**, 157 (1990).

[16] D. M. Haaland, Carbon **14**, 357 (1976).

[17] V. N. Korobenko, A. I. Savvatimski, and R. Cheret, Int. J. Thermophys. **20**, 1247 (1999).

[18] A. M. Kondratyev, V. N. Korobenko, and A. D. Rakhel, Carbon **100**, 537 (2016).

[19] A. M. Kondratyev, V. N. Korobenko, and A. D. Rakhel, J. Phys. Condens. Matter **28**, 265501 (2016).

[20] V. N. Korobenko and A. D. Rakhel, Int. J. Thermophys. **20**, 1257 (1999).

[21] L. M. Barker and R. E. Hollenbach J. Appl. Phys. **41**, 4208 (1970).

[22] G. A. Bergman et al., Tables of Standard Reference Data, GSSSD 25-90 (Izdatel'stvo Standartov, Moscow, 1991).

[23] M. W. Chase, Jr., J. L. Curnutt, J. R. Downey, Jr., R. A. McDonald, A. N. Syverud, and E. A. Valenzuela, J. Phys. Chem. Ref. Data **11**, 695 (1982).

[24] W. C. Morgan, Carbon **10**, 73 (1972).

[25] Y. S. Touloukian, R. K. Kirby, R. E. Taylor, and T. Y. R. Lee, Thermal Expansion, Nonmetallic Solids, Thermophysical Properties of Matter (IFI/Plenum, New York, 1977), Vol. 13.

[26] See Supplemental Material at http://link.aps.org/supplemental/10.1103/PhysRevLett.122.175702 for the table which contains the data presented in Figs. 2–4 for the four representing experiments as well as the measured dependence of the density of liquid carbon on pressure presented in Fig. 5.

[27] I. L. Shabalin, Ultra-High Temperature Materials I (Springer, Science+Business Media Dordrecht, 2014).

[28] M. Togaya, Phys. Rev. Lett. **79**, 2474 (1997).

[29] G. I. Kerley and L. Chhabildas, Sandia National Laboratories Report No. SAND2001-2619 2001.

[30] Karl A. Gschneidner, Solid State Phys. **16**, 275 (1964).

[31] A. M. Kondratyev, V. N. Korobenko, and A. D. Rakhel, J. Exp. Theor. Phys. **127**, 1074 (2018).

[32] M. French and T. R. Mattsson, J. Appl. Phys. **116**, 013510 (2014).

[33] J. P. Perdew, K. Burke, and M. Ernzerhof, Phys. Rev. Lett. **77**, 3865 (1996).